

A Method for Designing Three-Dimensional Configurations with Prescribed Skin Friction

S G Lekoudis,* N L Sankar,† and S F Radwan‡

Georgia Institute of Technology

Atlanta, Georgia

Nomenclature

| | |
|----------|--|
| c_f | = skin friction coefficient |
| U, W | = local boundary-layer velocity components in the x and z directions, respectively |
| δ | = increment during iterations |

Subscripts

| | |
|----------|--|
| e | = local boundary-layer edge conditions |
| x | = direction of local chord |
| z | = local spanwise direction |
| o | = values from previous iteration |
| ∞ | = freestream |

Introduction

THIS note addresses the viscous design problem for three-dimensional geometries. Close to the body surface the flow is treated as a boundary layer. The design is created as follows. The skin friction distribution is the target, used as input in an inverse boundary-layer calculation. The resulting pressure distribution is used as the input for an inverse potential flow calculation that generates the surface geometry.

The method described is based on inverse boundary layer calculations. The input is the skin friction coefficient and the output the pressure distribution. Solutions of the three-dimensional boundary-layer equations in the inverse mode have appeared recently in the literature.^{1,3} The solutions described herein are based on the method described in Ref 2. Anisotropic eddy viscosity is used for closure.

Inverse Boundary-Layer Scheme

The boundary layer scheme used is a modification to the one reported in Ref 2; thus, only the modification is described.

If c_{fx} and c_{fz} denote the local vector skin friction components in the x and z directions, respectively, and c_{fx}^* and c_{fz}^* the target values, a Taylor expansion gives the following relations:

$$c_{fx} = c_{fx}^* + \frac{\partial c_{fx}}{\partial U_e} \Delta U_e + \frac{\partial c_{fx}}{\partial W_e} \Delta W_e \quad (1a)$$

$$c_{fz} = c_{fz}^* + \frac{\partial c_{fz}}{\partial U_e} \Delta U_e + \frac{\partial c_{fz}}{\partial W_e} \Delta W_e \quad (1b)$$

Presented as Paper 84-0526 at the AIAA 22nd Aerospace Sciences Meeting, Reno, Nev., Jan. 9-12, 1984; received March 19, 1984; revision received May 22, 1984. Copyright © 1984 by S. G. Lekoudis. Published by the American Institute of Aeronautics and Astronautics with permission.

*Associate Professor, School of Aerospace Engineering, Member AIAA.

†Senior Research Engineer, School of Aerospace Engineering, Member AIAA.

‡Graduate Research Assistant, School of Aerospace Engineering, Student Member AIAA.

Equations (1) assume some proximity of the local values of the skin friction with the target values. In practice this proximity is obtained by using the velocity components of the previous location as initial guesses. From Eqs (1) one can solve for ΔU_e and ΔW_e and obtain

$$\Delta U_e = \left[(c_{fx} - c_{fx}^*) \frac{\partial c_{fx}}{\partial W_e} - (c_{fz} - c_{fz}^*) \frac{\partial c_{fx}}{\partial W_e} \right] / \left[\frac{\partial c_{fx}}{\partial U_e} - \frac{\partial c_{fz}}{\partial W_e} \frac{\partial c_{fx}}{\partial U_e} \right] \quad (2a)$$

$$\Delta W_e = \left[(c_{fx} - c_{fx}^*) \frac{\partial c_{fx}}{\partial U_e} - (c_{fx} - c_{fx}^*) \frac{\partial c_{fz}}{\partial U_e} \right] / \left[\frac{\partial c_{fx}}{\partial U_e} \frac{\partial c_{fz}}{\partial W_e} - \frac{\partial c_{fx}}{\partial W_e} \frac{\partial c_{fz}}{\partial U_e} \right] \quad (2b)$$

Equations (2) are used to obtain the increments in the components of the freestream velocity during the iteration procedure. This method of computing the inverse boundary layer amounts to solving the direct problem iteratively until the desired boundary condition is achieved. It was decided not to use the skin friction directly as a boundary condition, since that would have resulted in solving the boundary-layer equations with all conditions at the wall.

Numerical Procedure

The inverse potential flow method used is similar to the procedure described in Ref 4. The procedure can be used to design wing alone configurations at subsonic and transonic speeds. Several applications of this procedure are given in Ref. 4.

The partial derivatives of c_{fx} and c_{fz} in Eqs (1) were evaluated using increments ΔU_e and ΔW_e with δ controlled from input. Convergence was judged by the percentage changes in both velocities (U_e, W_e) and skin friction coefficients (c_{fx}, c_{fz}). The boundary layer equations then were both solved in the direct mode, three times per iteration, and $\partial c_{fx}/\partial U_e$, $\partial c_{fx}/\partial W_e$, $\partial c_{fz}/\partial U_e$, $\partial c_{fz}/\partial W_e$ were computed using a first order finite difference approximation. For

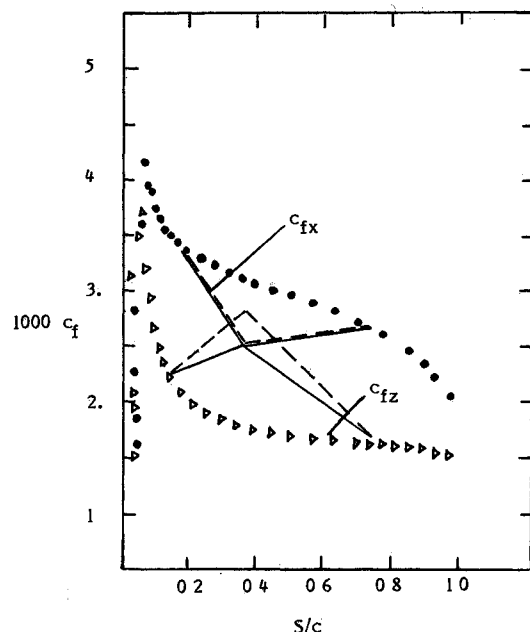


Fig. 1 Original (●, ▲) and imposed target (—, - - -) distributions of the skin friction.

example, if U_{e0} and W_{e0} were the current values of the freestream velocity components, and c_{fx1} and c_{fz1} the current values of the skin friction, a new calculation was performed with $U_{e0}(1+\delta)$ and W_{e0} as the freestream velocity components. This resulted in new c_{fx2} and c_{fz2} . Then

$$\frac{\partial c_{fx}}{\partial U_e} = \frac{c_{fx2} - c_{fx1}}{\delta U_{e0}} \quad (3)$$

$$\frac{\partial c_{fz}}{\partial U_e} = \frac{c_{fz2} - c_{fz1}}{\delta U_{e0}} \quad (4)$$

The same procedure was used for the $\partial c_f / \partial W_e$ derivatives and the velocities were updated using Eqs. (2) and (3) as follows:

$$U_e = U_{e0} + \Delta U_e \quad (5)$$

$$W_e = U_{e0} + \Delta W_e \quad (6)$$

In Ref. 2, where the input displacement thickness was translated into a boundary condition for the inverse calculations, upwind differencing of the convection terms was found necessary in order to obtain smooth solutions. In this work, where the input skin friction was approached iteratively, there was no need for upwinding. This may be due to the fact that the input boundary condition was achieved only within a prescribed tolerance.

Discussion of Results

A large aspect ratio transport wing was selected as the basic configuration. The wing had a sweep of 25 deg at the quarter chord, an aspect ratio of 8, and a taper ratio of 0.4. The calculations were made for a unit Reynolds number of 10^6 . The streamwise length of the wing root was 5.78 units long. The freestream Mach number used (0.15) makes the error due to the incompressible flow assumptions in the boundary layer very small.

For reasons of simplicity, and because the procedure does not include wake calculations, the target skin friction was prescribed only on part of the upper surface of the wing. The leading- and trailing edge regions were excluded. The boundary layer was solved on all 22 span stations, and the solution points on the surface were chosen to coincide with the locations where the solution is provided from the potential flow code. The local sweep was used, and for a wing with the characteristics mentioned previously, the infinite swept wing assumptions were reasonable to make. The surface coordinate S is measured from the leading edge line and on the airfoil normal to the leading edge. Since the leading and trailing edge regions were excluded, the curvature terms were not included in the boundary layer calculations through the metrics. The length c is the local chord length of the airfoil normal to the leading edge.

The boundary layer was tripped at a fixed point after the leading edge at approximately the location of the peak suction close to $S/c = 0.05$. In the inverse mode the calculations started at a fixed streamwise point close to $S/c = 0.16$. The direct mode was used up to that point. The isotropic eddy viscosity was used in all the cases.

The design was performed as follows. Excluding a region around the midchord of the upper surface, the skin friction values, and, therefore, the pressure, were kept unchanged and equal to the values computed from the direct mode on the wing. Figure 1 shows the imposed linear variation of c_{fx} and c_{fz} . It raises the c_{fz} and lowers the c_{fx} values in the region approximately $0.16 < S/c < 0.74$ on the upper surface. As expected the computed components U_e and W_e of the local freestream velocity follow the trend of the skin friction values and are shown in Fig. 2. This imposed rotation of the skin friction vector in the outboard spanwise direction may be

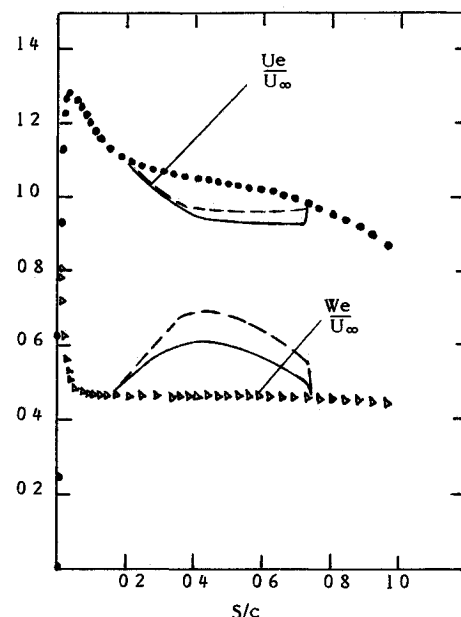


Fig. 2 Original (●, ▽) and resulting (—, - - -) edge velocity components

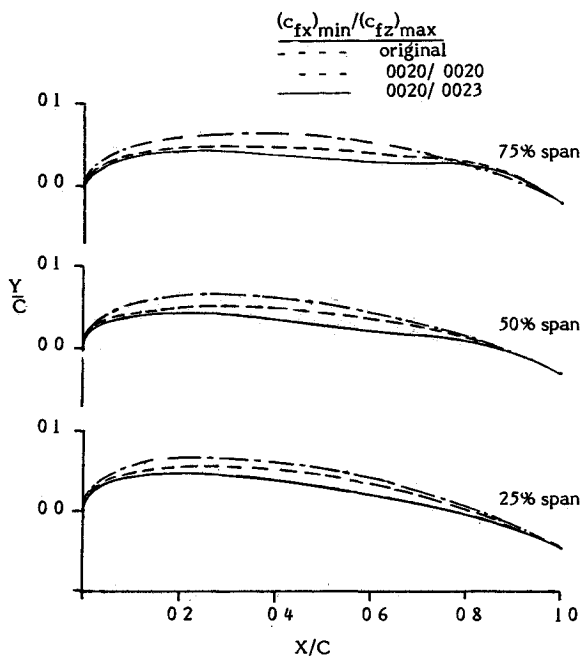


Fig. 3 Original and redesigned airfoil sections (upper surface) at different span locations.

accomplished without excessive thickening of the boundary layer. This turning of the skin friction vector reduces its drag producing component. Note that for two dimensional or axisymmetric bodies this mechanism of drag reduction does not work. While prescribing target skin friction, care must be taken to avoid excessive turning of the skin friction vector, leading to separation.

The pressure distributions show the effect of the imposed skin friction. Because no effort was made to prescribe a target skin friction so that the new and original pressures were joined smoothly the following behavior is observed. A discontinuity in the pressure distribution is generated at approximately $S/c \approx 0.74$. The inverse potential code predicted a somewhat smoother pressure distribution as it should, and produced airfoils with an abrupt change of profile slope at that location.

The upper surface of the redesigned wing sections at the 25% and 75% span locations are shown in Fig 3. There is a flattening of the upper surface similar to that observed in high lift airfoils.⁷ As previously mentioned, the sudden acceleration at $S/c \approx 0.74$ produced a discontinuity of the profile slope at that location. It was not possible to impose the target skin friction, shown in Fig 2, on the whole upper surface of the wing. When this was done, the design pressures failed to match the target close to the wing tip. Therefore, starting at span station 17, and up to the last station (22) at the wing tip the design skin friction was the linear interpolation between the values at station 17 and the original values at the tip. This procedure generated design pressures close to the target for the entire wing.

Conclusion

The results presented are a very small sample of the possible choices; however, they demonstrate a viable procedure for solving the viscous design problem in three dimensional flow. Designs with strong viscous/inviscid interaction effects have to be attempted using the present method after the two inverse codes are coupled. It can be concluded that 1) the work extends ideas already applied in two-dimensional problems^{5,7} to the three dimensional case, and 2) the work can be used to design wings with a specified target skin friction. Therefore it can be used for designing for low drag, high lift, or avoidance of separation.

Acknowledgment

The first and last authors were supported by a grant from the Advanced Research Organization of the Lockheed Georgia Company.

References

- 1 Cousteix J and Houdeville R Singularities in Three Dimensional Turbulent Boundary Layer Calculations and Separation Phenomena' *AIAA Journal* Vol. 19 Aug 1981 pp 976 985
- 2 Radwan S F and Lekoudis S G Boundary Layer Calculations in the Inverse Mode for Incompressible Flows Over Infinite Swept Wings *AIAA Journal* Vol 22 June 1984 pp 737 743
- 3 Delery J M and Formery M J A Finite Difference Method for Inverse Solutions of 3 D Turbulent Boundary Layer Flow AIAA Paper 83 0301 1983
- 4 Burris C B Henery P H and Sankar N L Computational Aerodynamic Design of Advanced Transport Aircraft' AIAA Paper 83 1865 1983
- 5 Smith A M O Stokes T R and Lee R S Optimum Tail Shapes for Bodies of Revolution, *Journal of Hydraulics* Vol 15 No 1 4 1981 pp 67 73
- 6 Liebeck R H Design of Subsonic Airfoils for High Lift' *Journal of Aircraft* Vol 15 Sept. 1978 pp 547 561
- 7 Lissaman P B X Low Reynolds Number Airfoils *Annual Review of Fluid Mechanics* Vol 15 1983 pp 223 239

AERO-OPTICAL PHENOMENA—V 80

Edited by Keith G. Gilbert and Leonard J. Otten Air Force Weapons Laboratory

This volume is devoted to a systematic examination of the scientific and practical problems that can arise in adapting the new technology of laser beam transmission within the atmosphere to such uses as laser radar, laser beam communications, laser weaponry, and the developing fields of meteorological probing and laser energy transmission among others. The articles in this book were prepared by specialists in universities, industry and government laboratories both military and civilian, and represent an up to date survey of the field.

The physical problems encountered in such seemingly straightforward applications of laser beam transmission have turned out to be unusually complex. A high intensity radiation beam traversing the atmosphere causes heat up and breakdown of the air, changing its optical properties along the path, so that the process becomes a nonsteady interactive one. Should the path of the beam include atmospheric turbulence the resulting nonsteady degradation obviously would affect its reception adversely. An airborne laser system unavoidably requires the beam to traverse a boundary layer or a wake, with complex consequences. These and other effects are examined theoretically and experimentally in this volume.

In each case, whereas the phenomenon of beam degradation constitutes a difficulty for the engineer it presents the scientist with a novel experimental opportunity for meteorological or physical research and thus becomes a fruitful nuisance!

412 pp 6 x 9 illus \$30 00 Mem \$45 00 List

TO ORDER WRITE Publications Dept., AIAA, 1633 Broadway, New York, N Y 10019